

---

# Association of quantitative magnetic resonance imaging parameters with histological findings from MRI/ultrasound fusion prostate biopsy

Seyed Saeid Dianat, MD,<sup>1</sup> H. Ballentine Carter, MD,<sup>2,4</sup> Edward M. Schaeffer, MD,<sup>2,4</sup> Ulrike M. Hamper, MD,<sup>1,2</sup> Jonathan I. Epstein, MD,<sup>2,3,4</sup> Katarzyna J. Macura, MD<sup>1,2,4</sup>

<sup>1</sup>The Russell H. Morgan Department of Radiology and Radiological Science, The Johns Hopkins University, School of Medicine, Baltimore, Maryland, USA

<sup>2</sup>The James Buchanan Brady Urological Institute, The Johns Hopkins University, School of Medicine, Baltimore, Maryland, USA

<sup>3</sup>Department of Pathology, The Johns Hopkins University, School of Medicine, Baltimore, Maryland, USA

<sup>4</sup>The Sidney Kimmel Comprehensive Cancer Center, The Johns Hopkins University, School of Medicine, Baltimore, Maryland, USA

---

DIANAT SS, CARTER HB, SCHAEFFER EM, HAMPER UM, EPSTEIN JI, MACURA KJ. Association of quantitative magnetic resonance imaging parameters with histological findings from MRI/ultrasound fusion prostate biopsy. *Can J Urol* 2015;22(5):7965-7972.

**Introduction:** Purpose of this pilot study was to correlate quantitative parameters derived from the multiparametric magnetic resonance imaging (MP-MRI) of the prostate with results from MRI guided transrectal ultrasound (MRI/TRUS) fusion prostate biopsy in men with suspected prostate cancer.

**Materials and methods:** Thirty-nine consecutive patients who had 3.0T MP-MRI and subsequent MRI/TRUS fusion prostate biopsy were included and 73 MRI-identified targets were sampled by 177 cores. The pre-biopsy MP-MRI consisted of T2-weighted, diffusion weighted (DWI), and dynamic contrast enhanced (DCE) images. The association of quantitative MRI measurements with biopsy histopathology findings was assessed by Mann-Whitney U- test and Kruskal-Wallis test.

**Results:** Of 73 targets, biopsy showed benign prostate tissue in 46 (63%), cancer in 23 (31.5%), and atypia/high

grade prostatic intraepithelial neoplasia in four (5.5%) targets. The median volume of cancer-positive targets was 1.3 cm<sup>3</sup>. The cancer-positive targets were located in the peripheral zone (56.5%), transition zone (39.1%), and seminal vesicle (4.3%). Nine of 23 (39.1%) cancer-positive targets were higher grade cancer (Gleason grade > 6).

Higher grade targets and cancer-positive targets compared to benign lesions exhibited lower mean apparent diffusion coefficient (ADC) value (952.7 < 1167.9 < 1278.9), and lower minimal extracellular volume fraction (ECF) (0.13 < 0.185 < 0.213), respectively. The difference in parameters was more pronounced between higher grade cancer and benign lesions.

**Conclusions:** Our findings from a pilot study indicate that quantitative MRI parameters can predict malignant histology on MRI/TRUS fusion prostate biopsy, which is a valuable technique to ensure adequate sampling of MRI-visible suspicious lesions under TRUS guidance and may impact patient management. The DWI-based quantitative measurement exhibits a stronger association with biopsy findings than the other MRI parameters.

**Key Words:** prostate cancer, multiparametric MRI, ultrasonography, biopsy

---

## Introduction

Histologic upgrading of prostate cancer occurs in at least 25% of patients on prostatectomy histopathology, which

is an inherent problem associated with standard random transrectal ultrasound (TRUS)-guided prostate biopsy for men with clinical suspicion of prostate cancer.<sup>1,2</sup> This is a major challenge in the management of men considering active surveillance (AS).

The other limitation of standard TRUS biopsy is the problem of undersampling sites far from the needle access such as the anterior aspect of the gland. This puts patients with persistently elevated prostate-specific antigen (PSA) but negative prior biopsies and patients on AS at risk of undertreatment and may lead to adverse disease outcome.<sup>3</sup>

Accepted for publication April 2015

Address correspondence to Dr. Katarzyna J. Macura, The Russell H. Morgan Department of Radiology and Radiological Science, The Johns Hopkins University, School of Medicine, 601 N. Caroline Street, JHOC 3140C, Baltimore, MD 21287 USA

Multiparametric prostate MRI (MP-MRI) has been increasingly utilized for AS of prostate cancer as well as management of men with suspected prostate cancer but negative or atypical findings on standard biopsies. MP-MRI has a favorable correlation with prostatectomy histopathology findings.<sup>4</sup> Targeted prostate biopsy is increasingly considered to be an adjunct to standard TRUS biopsy and may decrease the risk of tumor upgrading on prostatectomy specimen compared to detection based on TRUS biopsy alone.<sup>5</sup> MR-identified lesions are targeted either directly through the “in-bore” biopsy within the MR scanner, or indirectly by fusing MR images to real-time TRUS. Targeted biopsy through MR/TRUS fusion is beneficial regarding the feasibility, time, and cost.<sup>6,7</sup> Assessment of functional parameters, including diffusion-weighted imaging (DWI) and dynamic contrast-enhanced (DCE) MRI, substantially improves characterization and localization of prostate cancer in most of the clinical settings, as well as differentiation between benign and malignant pathologies visualized on T2-weighted images.<sup>8-10</sup>

Malignant lesions typically have a high cellular density and disorganized extracellular architecture that impede water molecule diffusion leading to restricted diffusion as measured by low apparent diffusion coefficient (ADC) value.<sup>11</sup> Furthermore, the ADC value is negatively correlated with tumor grade on prostatectomy specimen.<sup>12,13</sup> However, there is some overlap for ADC values between benign and malignant lesions.

Alterations in tumor vasculature such as tumor angiogenesis, higher permeability, vascular size heterogeneity, and disorganized branching are recognized by pharmacokinetic assessment in DCE-MRI.<sup>14</sup> The quantitative measures of DCE-MRI have not been widely studied in relation to histology findings.

In the present study, we evaluated the association of quantitative MRI parameters with biopsy findings from MRI/TRUS fusion prostate biopsy in men with MRI-visible suspicious prostate lesions. In this pilot study, we used a novel approach to MRI-TRUS fusion, in terms of ultrasound platform, fusion software, and biopsy operators, and the study is unique as it focuses on quantitative assessment of MRI parameters for biopsy target characterization.

## Materials and methods

### *Study design and population*

A cohort of 39 consecutive patients with clinical and/or biochemical suspicion of prostate cancer who

had 3.0T MP-MRI at our institution and underwent MRI/TRUS fusion targeted prostate biopsy between November 2011 and December 2013 were included in this retrospective HIPAA compliant study with a waiver of the consent based on the institutional review board approval. We included 24 men with high PSA and negative prior biopsies, 9 men in AS, 5 men for pre-treatment evaluation, and 1 man with post-brachytherapy biochemical recurrence.

### *MP-MRI protocol*

MP-MRIs were performed on 3.0T MR scanner and consisted of T2W, DWI, and DCE images. The MP-MRI was performed as previously described.<sup>15</sup> Images were acquired using the surface body matrix coil without the endorectal coil in 30 patients (76.9%) and with endorectal coil in 9 patients. MRI-suspicious lesions were reported on per sextant localization scheme and subsequently were targeted during the MRI/TRUS fusion biopsy.

### *MR/TRUS fusion biopsy procedure*

MR images were reviewed before the biopsy procedure by the radiologist. To perform the targeted biopsy, MRI data were imported from the picture archiving and communication system (PACS) into the Volume Navigation (VNav) software of the GE Healthcare LOGIQE9 US unit (GE Healthcare). An electromagnetic tracking device, positioned over the patient's pelvis, and the fusion software on US unit registered the real-time position of the endorectal ultrasound probe and allowed the fusion software to anatomically co-register the real-time images acquired on US unit during scanning with previously imported MRI datasets.

Once a transverse plane of the prostate on TRUS was locked to correspond to the MRI axial plane (lock plane), in a next step a common anatomical reference point in both the live TRUS and MRI dataset needed to be defined. During live scanning by an experienced sonographer and guided by the attending radiology physician, TRUS anatomical points were chosen, i.e. urethra at apex, cystic lesions, or BPH nodules in the transition zone and subsequently the same anatomical reference point(s) were documented and locked (lock point) on the MRI dataset. Once the scanning plane and at least two anatomical points were locked on TRUS and MRI, live ultrasound images and MRI dataset were synchronized. The navigational software allowed for synchronous movement of the US probe placed in the rectum with T2W images (or any MRI imaging sequence chosen), displayed on the US screen during the real-time imaging. Position displayed on MRI could be adjusted in the 3D volume to correspond

TABLE 1. Comparison of quantitative MR parameters of targets between different biopsy histopathology findings

	Benign targets <sup>†</sup> (n = 50)	Gleason 6 targets (n = 14)	Higher grade (Gleason > 6) cancer-positive targets (n = 9)	p value
Mean T2W SI	282.5 ± 90.5	274.5 ± 85	230.9 ± 109.3	0.32
Mean T2W SI (normalized)	0.64 ± 0.18	0.67 ± 0.13	0.63 ± 0.20	0.65
Max T2W SI	517.8 ± 146.2	499.4 ± 124.8	451.4 ± 188.7	0.33
Min T2W SI	129.6 ± 69.8	124 ± 63.4	90.6 ± 80.7	0.21
SD T2W SI	60.2 ± 17.8	62.9 ± 16.4	57.6 ± 28.2	0.57
Mean ADC	1278.9 ± 180.2	1167.9 ± 209.1	952.7 ± 308.3	0.003
Mean ADC (normalized)	0.77 ± 0.11	0.72 ± 0.15	0.60 ± 0.15	0.008
Median ADC	1267.9 ± 179.6	1150.4 ± 221.7	932.6 ± 317.9	0.002
Median ADC (normalized)	0.76 ± 0.11	0.72 ± 0.15	0.58 ± 0.16	0.008
Max ADC	1921.9 ± 263.1	1846.1 ± 234.6	1836.3 ± 359.1	0.58
Max ADC (normalized)	0.91 ± 0.12	0.95 ± 0.23	0.93 ± 0.16	0.96
Min ADC	731.7 ± 340.2	613.7 ± 322.8	365.4 ± 299.4	0.01
Min ADC (normalized)	0.66 ± 0.34	0.53 ± 0.30	0.29 ± 0.18	0.003
SD ADC	248 ± 84.9	247.2 ± 67.8	271.8 ± 67.3	0.73
Mean K <sup>trans</sup>	5.32 ± 6.62	4.95 ± 5.66	6.41 ± 6.14	0.81
Mean K <sup>trans</sup> (normalized)	5.0 ± 8.86	4.92 ± 7.20	3.86 ± 3.40	0.70
Median K <sup>trans</sup>	3.98 ± 6.92	2.62 ± 2.98	3.07 ± 3.02	0.86
Median K <sup>trans</sup> (normalized)	4.04 ± 5.82	3.25 ± 4.77	3.82 ± 4.60	0.62
Max K <sup>trans</sup>	25.53 ± 20.18	24.31 ± 21.77	29.15 ± 24.55	0.75
Max K <sup>trans</sup> (normalized)	15.91 ± 58.80	17.90 ± 43.72	5.75 ± 8.56	0.85
Min K <sup>trans</sup>	0.35 ± 0.41	0.21 ± 0.16	0.159 ± 0.2	0.10
Min K <sup>trans</sup> (normalized)	2.38 ± 3.72	1.76 ± 2.12	1.08 ± 1.40	0.49
SD K <sup>trans</sup>	5.16 ± 5.07	5.65 ± 6.12	7.4 ± 7	0.82
Mean EVF	0.513 ± 0.137	0.479 ± 0.136	0.412 ± 0.1	0.13
Mean EVF (normalized)	1.16 ± 0.41	1.25 ± 0.49	1.12 ± 0.36	0.92
Median EVF	0.499 ± 0.147	0.462 ± 0.138	0.397 ± 0.103	0.15
Median EVF (normalized)	1.19 ± 0.49	1.25 ± 0.44	1.11 ± 0.37	0.83
Max EVF	0.924 ± 0.118	0.867 ± 0.177	0.916 ± 0.145	0.39
Max EVF (normalized)	1.21 ± 0.52	1.40 ± 0.71	1.36 ± 0.53	0.30
Min EVF	0.213 ± 0.094	0.185 ± 0.079	0.13 ± 0.036	0.02
Min EVF (normalized)	1.11 ± 0.61	1.09 ± 0.45	0.96 ± 0.60	0.60
SD EVF	0.144 ± 0.035	0.14 ± 0.035	0.138 ± 0.031	0.80
Mean K <sub>ep</sub>	10.17 ± 11.68	11.02 ± 13.76	16.1 ± 15.87	0.66
Mean K <sub>ep</sub> (normalized)	4.98 ± 11.38	3.30 ± 4.13	4.05 ± 4.0	0.70

Kruskal-Wallis test was used for assessment of statistical significance of intergroup difference. Data are shown as mean ± SD. SI = signal intensity; ADC = apparent diffusion coefficient; K<sup>trans</sup> = permeability rate; EVF = extracellular volume fraction; K<sub>ep</sub> = contrast efflux rate constant; <sup>†</sup>benign targets consisted of benign tissue, HGPIN or atypia in the targeted biopsy.

to the real-time US even in oblique planes. The targeted biopsies were performed in axial plane using 18-gauge core biopsy needles. The trajectory of the biopsy needle was recorded and exported to a PACS. The biopsy procedures were performed by a group of selected radiologists not only familiar with prostate anatomy but also experienced at routine TRUS biopsies.

### Post-biopsy image analysis

The quantitative MR measurements of targeted lesions were performed after targeted biopsy procedure. The analysis of the regions of interests (ROIs) was performed blindly per each target, without the knowledge of final biopsy result. Needle trajectories sampling the targets were reviewed from the saved screen shots of MRI/TRUS fusion targeted biopsy. Corresponding ROIs were drawn on T2W images and propagated to other MRI parameters using a computer-aided diagnosis (CAD) system (DynaCAD, Invivo, Gainesville, FL, USA). Additional ROI of normal region, i.e. contralateral, that corresponded to the location of targeted ROI was similarly drawn on T2W images. Tofts' two-compartment pharmacokinetic model was used for perfusion map generation and calculation of DCE parameters. The quantitative measurements including T2W signal intensity (SI), ADC,  $K^{trans}$  (forward volume transfer constant), EVF (extracellular volume fraction), and  $K_{ep}$  (reverse reflux rate constant) were stored for each individual target and the corresponding normal ROI. Normalized ratios were calculated by dividing the measures for targeted ROI to normal ROI for each target.

### Statistical analysis

The association of quantitative MR measurements with biopsy histopathology findings was assessed by Mann-Whitney U test and Kruskal-Wallis test. The Kruskal-Wallis test was used to determine presence of any statistical significance between biopsy finding groups (benign, Gleason 6 tumor, and higher grade tumor above Gleason 6). In case of statistical significance ( $p < 0.05$ ), multiple pairwise comparisons using Mann-Whitney U test with Bonferroni correction were performed. Statistical analysis was performed using the IBM Statistical Package for the Social Sciences (SPSS, version 20).

## Results

The median age of patients in this cohort was 66 years (range, 54-78). The median PSA level at the time of biopsy was 8.8 ng/mL (range, 2.2-36.2). The median MR-measured prostate volume was 60.1 cm<sup>3</sup> (19.7-199). A total of 73 MR-identified targets (median volume 0.73 cm<sup>3</sup>, range 0.18-6.96) were sampled by 177 cores.

Of 73 targets, biopsy showed benign prostate tissue in 46 (63%), cancer in 23 (31.5%), and atypia or high grade prostatic intraepithelial neoplasia in four (5.5%) targets. The median Gleason score of cancer-positive targets was 3 + 3 (range, 3 + 3 to 4 + 5). Higher grade cancer (Gleason score > 6) was identified in 9 of 23 (39.1%) cancer-positive targets; (G3 + 4, 5 targets; G4 + 3, 1 target; G4 + 4, 2 targets; and G4 + 5, 1 target). The cancer-positive targets were located in the peripheral zone (PZ) (56.5%), transition zone (TZ) (39.1%), and seminal vesicle (4.3%). The median volume of cancer-positive targets was 1.3 cm<sup>3</sup> (range, 0.18-6.96). Figure 1 shows an example of an anterior suspicious lesion in the transition zone in a patient with high PSA but three negative prior biopsies; MR/TRUS fusion biopsy demonstrated Gleason 3 + 3 prostate cancer.

Comparison of quantitative MR profile of targeted ROIs in three groups of benign, Gleason 6 cancer targets, and higher grade (Gleason score > 6) cancer targets are shown in Table 1. There was a significant difference between three groups in terms of mean ( $p = 0.003$ ), normalized mean ( $p = 0.008$ ), median ( $p = 0.002$ ), normalized median ( $p = 0.008$ ), minimal ( $p = 0.01$ ), and normalized minimal ( $p = 0.003$ ) measures of ADC value, and minimal measure for EVF value ( $p = 0.02$ ). Those parameters were not significantly different among benign and Gleason 6 tumor on

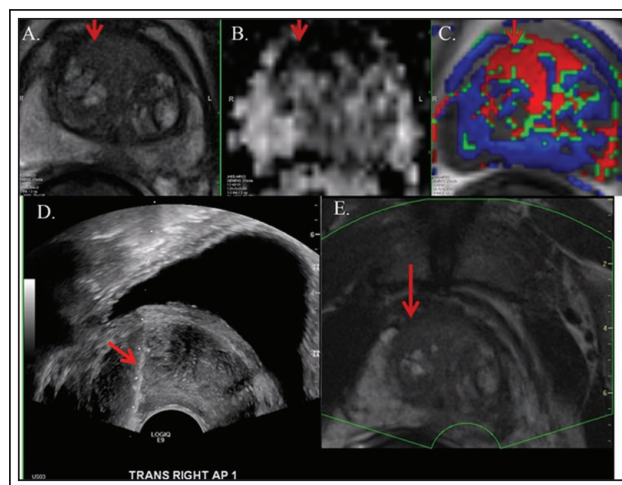


**Figure 1.** A 65-year-old man with elevated PSA and three negative prior TRUS biopsies of the prostate. MP-MRI shows (A) ill-defined T2W signal abnormality in the anterior aspect of the transition zone (arrow), (B) focally restricted diffusion (arrow) on ADC map, and (C) abnormal pharmacokinetic profile of early enhancement with quick washout (arrow) on post processed DCE color map. MR/TRUS fusion biopsy (D, E) revealed Gleason 3 + 3 prostate cancer.

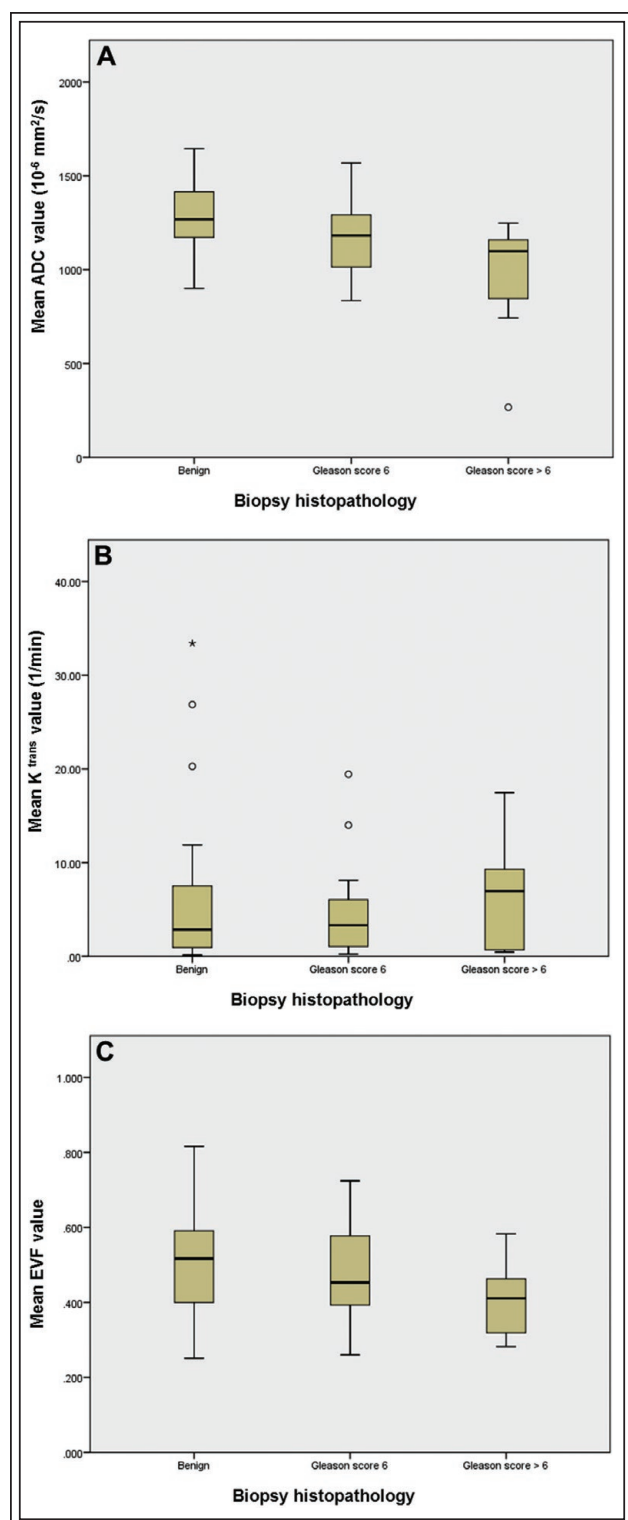


**Figure 2.** Boxplots of mean ADC value (A), mean  $K^{\text{trans}}$  value (B), and mean EVF value (C) show the trend between benign, Gleason score 6, and higher-grade (Gleason score > 6) prostate cancer pathology findings of MR/TRUS fusion targeted biopsies.

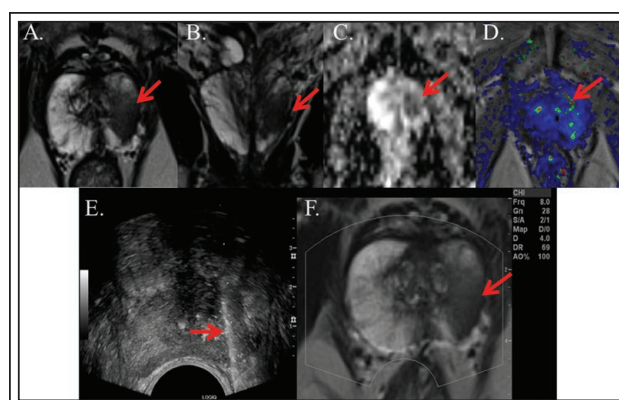


**Figure 3.** A 59-year-old man, biopsy-naïve, with elevated PSA and high PSA velocity (PSA increase from 4.1 to 7 in a year). MP-MRI shows highly suspicious findings on T2WI (A, B) and focally restricted diffusion on ADC map (C). Post processed DCE color map shows small focus of abnormal pharmacokinetic profile (D). Patient preferred MR/TRUS fusion targeted biopsy for follow up (E, F) and the biopsy sample showed Gleason 3 + 4 prostate cancer.

pairwise comparison. The difference was more profound between benign targets and higher grade (Gleason > 6) cancer targets. Mean, normalized mean, median, normalized median, minimal, and normalized minimal ADC values were significantly lower for higher grade (Gleason score > 6) cancer targets compared to those of benign targets ( $p = 0.001$ ,  $p = 0.002$ ,  $p = 0.001$ ,  $p = 0.002$ ,  $p = 0.006$ ,  $p = 0.001$ , respectively,  $p < 0.02$  for all parameters after Bonferroni correction). Pairwise comparison of the parameters between Gleason 6 and Gleason > 6 cancer targets showed only significant difference for normalized mean ADC ( $p = 0.03$ ) and minimal EVF ( $p = 0.05$ ), that are not significant after Bonferroni correction. Figure 2 shows the trend of low ADC, high  $K^{\text{trans}}$ , and low EVF between three groups of biopsy histopathology findings. Figure 3 shows the MP-MRI of a biopsy-naïve patient with elevated PSA level and highly suspicious T2W signal abnormality as well as focally restricted diffusion but with only a small focus of abnormal perfusion on DCE color map; the MR/TRUS fusion biopsy revealed Gleason 3 + 4 prostate cancer.

## Discussion

The important role of targeted prostate biopsy is substantiated in the management of several clinical scenarios; 1) low risk prostate cancer patients with clinical and/or biochemical suspicion of higher-grade

prostate cancer managed in AS, 2) patients with persistently elevated PSA level but negative prior prostate biopsies, and 3) patients demonstrating a suspicious lesion on post-treatment MRI who prefer a targeted rather than random biopsy. This study reports the performance of MR/TRUS fusion biopsy of the prostate by the radiology service in an outpatient setting. In our small cohort of consecutive patients with MRI-detected lesions, the cancer detection rate was 31.5%. Curative treatment was indicated in 11 of 39 (28.2%) patients based on targeted biopsy findings.

Quantitative surrogate of water molecule diffusivity on DWI, the ADC value, was the most useful MRI parameter for prediction of malignancy in the target lesions. The mean and median ADC values were shown as the useful and statistically significant parameter to distinguish prostate cancer from benign targets as well as higher grade prostate cancer from Gleason 6 prostate cancer targets. The comparison of standard deviation of ADC value among different targets showed similar dispersion of ADC values of ROI voxels in the three biopsy pathology groups. Recently, the average and 10<sup>th</sup> percentile ADC values were reported as the best quantitative MR parameters to differentiate prostate cancer from normal PZ using prostatectomy as the reference.<sup>16</sup> The 10<sup>th</sup> percentile ADC value is comparable to the minimal ADC value recorded in our study showing similar differentiating potential. The use of minimal as well as median ADC values in interpretation of ADC maps is beneficial to characterize sparse prostate cancer foci with intermixed benign prostate tissue.

The ADC value also aids in differentiation of prostate cancer from benign mimickers. Nagel et al reported that the ADC value can help to differentiate prostate cancer from prostatitis on MR-guided biopsy that may have similar appearance on T2W and DCE images. They reported a downward trend for the median ADC values from normal prostate tissue ( $1.22 \times 10^{-3} \text{ mm}^2/\text{sec}$ ), prostatitis ( $1.08 \times 10^{-3} \text{ mm}^2/\text{sec}$ ), low grade ( $0.88 \times 10^{-3} \text{ mm}^2/\text{sec}$ ), to high grade prostate cancer ( $0.88 \times 10^{-3} \text{ mm}^2/\text{sec}$ ); however, an overlap existed for the ADC value between the low and high grade prostate cancer.<sup>17</sup>

Targeting suspicious lesions based on the ADC map as the only functional MR parameter was not commonly reported. Watanabe et al studied the diagnostic yield of targeting lesions with restricted diffusion on 1.5T in patients with high or increasing PSA suspected of prostate cancer by employing the MR findings and cognitively correlating it to the echo pattern on real-time TRUS exam or clockwise sampling from the suspected segment on MRI in cases with no

visible hypoechoic lesion at the corresponding TRUS segment. There were significant differences in ADC values between cancer-positive and benign targets with ADC values less than  $1.35 \times 10^{-3} \text{ mm}^2/\text{sec}$  for prostate cancer targets. Although the ADC values seemed to have a downward trend for the increasing tumor grade, the ADC values were not significantly different.<sup>18</sup> In another study, authors showed a significantly higher cancer detection rate in patients with additional targeted biopsy based on the ADC map (70.1%) compared to the detection rate on the systematic biopsy in another group with lack of low ADC lesion (13.1%).<sup>19</sup>

Various ADC parameters such as mean,<sup>16,20-22</sup> median,<sup>13</sup> 10<sup>th</sup> percentile,<sup>16</sup> and 25<sup>th</sup> percentile<sup>23</sup> have been reported in different studies in correlation with prostate cancer Gleason grade. Recently, it was reported that the ADC entropy reflecting the lesion heterogeneity and ADC variability in the whole-lesion can be useful to differentiate the percentage of Gleason 4 pattern in Gleason 7 tumors; however, the mean ADC value was not significantly different in relation to the percentage of Gleason 4 pattern.<sup>24</sup> This may reflect lesion heterogeneity or tumor intermixed with benign tissue affecting the quantitative imaging of suspicious lesions.

In contrast, Nagarajan et al reported that the mean ADC value on 1.5T MRI could predict tumor aggressiveness in reference to prostatectomy pathology findings and was significantly different among Gleason 6, Gleason 3 + 4, and Gleason 4 + 3 prostate cancer.<sup>25</sup>

Furthermore, the mean ADC value was better ( $r = -0.55$ ) than TRUS-guided systematic biopsy ( $r = 0.042$ ) in terms of correlation with prostatectomy Gleason grade.<sup>12</sup> Recently, TRUS-guided biopsy of suspicious lesions on DWI and/or MR spectroscopy revealed a significantly higher cancer detection rate as compared to TRUS-guided random biopsy (65% versus 36.5%). Overall, targeted biopsy of suspicious lesions on MRI had a higher concordance rate with prostatectomy histology compared to TRUS-guided random biopsy histology in terms of the highest Gleason grade lesion (89.6% versus 72.9%).<sup>26</sup>

Few studies reported the correlation of prostate tissue histological characteristics with quantitative MR parameters. The ADC value was shown to have a negative correlation with tumor cellularity and proliferation.<sup>27</sup> The difference in tumor microstructure is recognized by significant difference in the ADC parameters among benign, low, and high grade prostate cancer in our study.

The association of quantitative DCE parameters with pathology and disease outcome is not well established.

The tumor vascular microenvironment typically has high vascular density with high permeability and low extracellular volume as a result of tumor neoangiogenesis; however, hypoxia induced by high cellular density may cause poorer perfusion and lower permeability. In our study, the only quantitative DCE parameter that could barely reach the level of significance between different targeted biopsy histologies was the minimal EVF. In another study, the quantitative MRI parameters of T2WI, ADC,  $K^{trans}$ , and  $V_e$  or EVF were reported to correlate with some histological features such as percentage area of nucleus, cytoplasm, and luminal space.<sup>28</sup> These histological features may reflect the tissue cellularity and microstructure organization affecting the difference of ADC value and EVF among different biopsy groups in our study.

Several authors have also reported that prostatic inflammation exhibited a pharmacokinetic profile very close to prostate cancer leading to the low specificity of DCE parameters to characterize prostate cancer. Furthermore, DCE exhibited a lower sensitivity compared to T2WI for characterization of prostate cancer.<sup>29</sup>

Qualitative assessment of T2WI using Prostate Imaging and Reporting Data System (PI-RADS) scoring has shown the highest predictive role for tumor detection on fusion biopsy followed by DWI and DCE; however, assessment of T2WI had a lower diagnostic performance for detection of clinically significance tumor (Gleason  $\geq 7$ ) in comparison with DWI and DCE.<sup>30</sup> Quantitative analysis of signal intensity (SI) on T2WI has not been extensively employed in prostate imaging. Our data showed that measurement of T2W SI was not predictive of cancer on targeted biopsies due to the heterogeneity of the lesions on T2WI and did not have any discriminatory potential for benign versus cancer targets; however, a lower T2W SI was observed with more unfavorable pathology finding. The T2W SI skewness is a quantitative measure of dark-to-bright pixels ratio and has been shown to differentiate prostate cancer from normal PZ tissue in reference to prostatectomy specimen (AUC of 0.86).<sup>16</sup> However, in our cohort, quantitative T2WI failed to differentiate prostate cancer from benign targets, which was evident by lack of significant difference on T2W SI measurements despite of similar SI dispersion of voxels as well as normalization of values.

This study has several limitations. First, this is a small cohort study of consecutive patients referred to the radiology ultrasound service for targeted prostate biopsy at our institution. In this pilot study we used a new fusion biopsy technique that had not yet been reported. Our study was designed for target analysis where 73 biopsied targets constituted our study sample

with per-target correlation between quantitative parameters from MRI and histopathology results from MRI/TRUS fusion prostate biopsy. Second, patients were from different risk groups affecting the cancer detection rate using targeted biopsy. However, by including consecutive patients in the sample, regardless of the referral indication, we were able to analyze targets ranging from benign to high-grade cancers. Third, subgroup analysis based on zonal location of lesions was not possible considering the small sample size. Fourth, full assessment of false-positive and false-negative ROIs was not possible in the absence of whole-mount prostatectomy histopathology as the reference standard. However, in our design the exact biopsy location documented during the biopsy procedure was used for anatomical correlation to pre-biopsy MP-MRI and therefore the quantitative markers derived from MRI corresponded closely to targets sampled for histopathology analysis.

## Conclusion

Our preliminary report from this pilot study indicates that when targeting suspicious prostate lesions using MRI/TRUS fusion prostate biopsy technique, on a novel platform, as described above, the ADC value serves as the best quantitative MR parameter to distinguish malignant from benign prostate tissue with a potential to differentiate high from low grade prostate cancer; however an overlap exists between malignant and benign tissue, as well as high grade and low grade prostate cancer. Therefore, prostate MRI protocols need to include DWI with ADC mapping to minimize the risk of tumor undergrading and missing prostate cancer particularly in men with high PSA but persistently negative standard TRUS biopsies and men managed with AS. Larger scale prospective studies are needed to validate our preliminary findings. □

---

## References

1. Carlson GD, Calvanese CB, Kahane H, Epstein JI Accuracy of biopsy Gleason scores from a large uropathology laboratory: use of a diagnostic protocol to minimize observer variability. *Urology* 1998;51(4):525-529.
2. Tilki D, Schlenker B, John M et al. Clinical and pathologic predictors of Gleason sum upgrading in patients after radical prostatectomy: results from a single institution series. *Urol Oncol* 2011;29(5):508-514.

## Association of quantitative magnetic resonance imaging parameters with histological findings from MRI/ultrasound fusion prostate biopsy

3. Hoeks CM, Schouten MG, Bomers JG et al. Three-tesla magnetic resonance-guided prostate biopsy in men with increased prostate-specific antigen and repeated, negative, random, systematic, transrectal ultrasound biopsies: detection of clinically significant prostate cancers. *Eur Urol* 2012;62(5):902-909.
4. Turkbey B, Mani H, Shah V et al. Multiparametric 3T prostate magnetic resonance imaging to detect cancer: histopathological correlation using prostatectomy specimens processed in customized magnetic resonance imaging based molds. *J Urol* 2011;186(5):1818-1824.
5. Siddiqui MM, Rais-Bahrami S, Truong H et al. Magnetic resonance imaging/ultrasound-fusion biopsy significantly upgrades prostate cancer versus systematic 12-core transrectal ultrasound biopsy. *Eur Urol* 2013;64(5):713-719.
6. Franiel T, Stephan C, Erbersdobler A et al. Areas suspicious for prostate cancer: MR-guided biopsy in patients with at least one transrectal US-guided biopsy with a negative finding--multiparametric MR imaging for detection and biopsy planning. *Radiology* 2011;259(1):162-172.
7. Sonn GA, Margolis DJ, Marks LS. Target detection: Magnetic resonance imaging-ultrasound fusion-guided prostate biopsy. *Urol Oncol* 2014;32(6):903-911.
8. Sato C, Naganawa S, Nakamura T et al. Differentiation of noncancerous tissue and cancer lesions by apparent diffusion coefficient values in transition and peripheral zones of the prostate. *J Magn Reson Imaging* 2005;21(3):258-262.
9. Kozlowski P, Chang SD, Jones EC, Berean KW, Chen H, Goldenberg SL Combined diffusion-weighted and dynamic contrast-enhanced MRI for prostate cancer diagnosis--correlation with biopsy and histopathology. *J Magn Reson Imaging* 2006;24(1):108-113.
10. Engelbrecht MR, Huisman HJ, Laheij RJ et al. Discrimination of prostate cancer from normal peripheral zone and central gland tissue by using dynamic contrast-enhanced MR imaging. *Radiology* 2003;229(1):248-254.
11. Dianat SS, Carter HB, Macura KJ. Performance of multiparametric magnetic resonance imaging in the evaluation and management of clinically low-risk prostate cancer. *Urol Oncol* 2014;32(1):39 e31-10.
12. Bittencourt LK, Barentsz JO, de Miranda LC, Gaspardo EL. Prostate MRI: diffusion-weighted imaging at 1.5T correlates better with prostatectomy Gleason Grades than TRUS-guided biopsies in peripheral zone tumours. *Eur Radiol* 2012;22(2):468-475.
13. Hambrock T, Somford DM, Huisman HJ et al. Relationship between apparent diffusion coefficients at 3.0-T MR imaging and Gleason grade in peripheral zone prostate cancer. *Radiology* 2011;259(2):453-461.
14. Bonekamp D, Jacobs MA, El-Khouli R, Stoianovici D, Macura KJ. Advancements in MR imaging of the prostate: from diagnosis to interventions. *Radiographics* 2011;31(3):677-703.
15. Mullins JK, Bonekamp D, Landis P et al. Multiparametric magnetic resonance imaging findings in men with low-risk prostate cancer followed using active surveillance. *BJU Int* 2013;111(7):1037-1045.
16. Peng Y, Jiang Y, Yang C et al. Quantitative analysis of multiparametric prostate MR images: differentiation between prostate cancer and normal tissue and correlation with Gleason score--a computer-aided diagnosis development study. *Radiology* 2013;267(3):787-796.
17. Nagel KN, Schouten MG, Hambrock T et al. Differentiation of prostatitis and prostate cancer by using diffusion-weighted MR imaging and MR-guided biopsy at 3 T. *Radiology* 2013;267(1):164-172.
18. Watanabe Y, Nagayama M, Araki T et al. Targeted biopsy based on ADC map in the detection and localization of prostate cancer: a feasibility study. *J Magn Reson Imaging* 2013;37(5):1168-1177.
19. Watanabe Y, Terai A, Araki T et al. Detection and localization of prostate cancer with the targeted biopsy strategy based on ADC map: a prospective large-scale cohort study. *J Magn Reson Imaging* 2012;35(6):1414-1421.
20. Vargha HA, Akin O, Franiel T et al. Diffusion-weighted endorectal MR imaging at 3 T for prostate cancer: tumor detection and assessment of aggressiveness. *Radiology* 2011;259(3):775-784.
21. Turkbey B, Shah VP, Pang Y et al. Is apparent diffusion coefficient associated with clinical risk scores for prostate cancers that are visible on 3-T MR images? *Radiology* 2011;258(2):488-495.
22. Oto A, Yang C, Kayhan A et al. Diffusion-weighted and dynamic contrast-enhanced MRI of prostate cancer: correlation of quantitative MR parameters with Gleason score and tumor angiogenesis. *AJR Am J Roentgenol* 2011;197(6):1382-1390.
23. Kobus T, Vos PC, Hambrock T et al. Prostate cancer aggressiveness: in vivo assessment of MR spectroscopy and diffusion-weighted imaging at 3 T. *Radiology* 2012;265(2):457-467.
24. Rosenkrantz AB, Triolo MJ, Melamed J, Rusinek H, Taneja SS, Deng FM. Whole-lesion apparent diffusion coefficient metrics as a marker of percentage Gleason 4 component within Gleason 7 prostate cancer at radical prostatectomy. *J Magn Reson Imaging* 2015;41(3):708-714.
25. Nagarajan R, Margolis D, Raman S et al. Correlation of Gleason scores with diffusion-weighted imaging findings of prostate cancer. *Adv Urol* 2012;2012:374805.
26. Zhang J, Xiu J, Dong Y et al. Magnetic resonance imaging directed biopsy improves the prediction of prostate cancer aggressiveness compared with a 12-core transrectal ultrasound-guided prostate biopsy. *Mol Med Rep* 2014;9(5):1989-1997.
27. Wang XZ, Wang B, Gao ZQ et al. Diffusion-weighted imaging of prostate cancer: correlation between apparent diffusion coefficient values and tumor proliferation. *J Magn Reson Imaging* 2009;29(6):1360-1366.
28. Langer DL, van der Kwast TH, Evans AJ et al. Prostate tissue composition and MR measurements: investigating the relationships between ADC, T2, K(trans), v(e), and corresponding histologic features. *Radiology* 2010;255(2):485-494.
29. Ocak I, Bernardo M, Metzger G et al. Dynamic contrast-enhanced MRI of prostate cancer at 3 T: a study of pharmacokinetic parameters. *AJR Am J Roentgenol* 2007;189(4):849.
30. Roethke MC, Kuru TH, Schultze S et al. Evaluation of the ESUR PI-RADS scoring system for multiparametric MRI of the prostate with targeted MR/TRUS fusion-guided biopsy at 3.0 Tesla. *Eur Radiol* 2014;24(2):344-352.